

Photon lifetime correlated increase of Raman scattering and third-harmonic generation in silicon nanowire arrays

S V Zobotnov^{1,2}, M M Kholodov¹, V A Georgobiani¹, D E Presnov¹,
L A Golovan¹ and P K Kashkarov^{1,2}

¹ Physics Department, Lomonosov Moscow State University, 1/2 Leninskie Gory, Moscow 119991, Russia

² Moscow Institute of Physics and Technology, 9 Institutsky Lane, 141700 Dolgoprudny, Moscow Region, Russia

E-mail: zobotnov@physics.msu.ru

Received 11 June 2015, revised 30 July 2015

Accepted for publication 13 January 2016

Published 11 February 2016



Abstract

Light propagation in silicon nanowire layers is studied via Raman scattering, third-harmonic generation and cross-correlation function measurements. The studied silicon nanowire arrays are characterized by a wire diameter of 50–100 nm and a layer thickness ranging from 0.2–16 μm . These structures are mesoscopic for light in the visible and near infrared ranges. The Raman signal increases monotonically with layer thickness increases at a 1.064 μm pump wavelength. The Stokes component for silicon nanowire arrays with a thickness larger than 2 μm exceeds that for crystalline silicon by more than an order. At the mentioned thicknesses, an increase is also registered for the third-harmonic signal, one that is up to fourfold greater than that for crystalline silicon for a 1.25 μm pump wavelength. Measurements of cross-correlation functions for the scattered photons evidence the significant photon lifetime increase in the silicon nanowire layers at their thickness increase. This fact can be connected with multiple scattering inside the studied mesoscopic structures and the increase of the interaction length for the Raman and third-harmonic generation processes.

Keywords: silicon nanowires, Raman scattering, third-harmonic generation, cross-correlation function

(Some figures may appear in colour only in the online journal)

1. Introduction

Silicon photonics now successfully combines the achievements of the most highly developed semiconductor and optics technologies [1]. In particular, arrays of silicon nanowires (SiNWs) are attracting more and more interest from researchers [2] because of their great potential for applications in photovoltaics [3–5], optoelectronics [6, 7], and photonics [8, 9].

Typically, the arrays consist of monocrystalline silicon (c-Si) wires that are 20–200 nm in diameter and 1–200 μm in length. These structures have been known since the mid-1960s [10], but the novel, simple and inexpensive technique of metal-assisted chemical etching (MACE) [11–13] brought

new opportunities for the formation of SiNWs. This technique employs a two-stage chemical process: in the first, silver nanoparticles are chemically deposited at the c-Si surface, and in the second, these act as catalysts, controlling the macropore etching in the c-Si. Further, the silver nanoparticles can be removed by rinsing the sample in nitric acid (HNO_3). MACE allows straight or zigzag SiNWs to be formed [11]. The very interesting features of the formed SiNW arrays are: (i) visible photoluminescence (PL), caused by the occurrence of Si nanocrystals during the etching process at the nanowire walls [12, 14]; (ii) extremely low total reflection (up to 1% in the visible range) [15–17]; and (iii) highly efficient interband PL and Raman scattering compared with c-Si [14, 16, 17].

The latter two effects are often connected with the enlargement of the photon path in scattering media such as SiNW arrays [16–19]. This process brings about redistribution of the local fields. In turn, the local-field variation at the wavelength scale can increase the efficiency of nonlinear-optical processes, such as second-harmonic generation [20, 21], coherent anti-Stokes Raman scattering [22], and light self-action [23]. Effective third-harmonic (TH) generation has also been observed in SiNWs [24]. However, the authors of this last work explain the intense TH emission from SiNWs in terms of the relatively large third-order susceptibility of silicon in comparison with other materials, such as CdS, TiO₂, and Au. To the best of our knowledge, no other studies concerning TH generation in SiNWs have yet been carried out. We forecast that the efficiency of this process in SiNWs may exceed that for c-Si, because of multiple scattering, local field redistribution, and the associated photon lifetime increase in the aforementioned mesoscopic structures. Earlier, such an effect was obtained for mesoporous silicon [25].

It would be very instructive to compare the results of experiments on nonlinear-optical processes, such as TH generation, with those of the linear optical processes of spontaneous Raman scattering studied earlier for SiNW arrays. Since the efficiency of the processes in scattering media such as SiNW arrays depends strongly on the photon lifetime in our assumption, we vary the thickness of the structures in our experiments. In our paper special attention is paid to the measurement and analysis of cross-correlation functions. It should also be noted that photon lifetime measurements have not yet been carried out for SiNW arrays.

2. Materials and methods

The SiNW arrays for our experiments were fabricated on *p*-type 12 Ω·cm (100)-oriented c-Si wafers using the MACE method. First, the wafers were dipped in 49% HF solution for 1 min to remove native oxide coverage. Then, Ag nanoparticles were deposited onto the surface of the substrates by immersing them in an aqueous solution of 0.02 M AgNO₃ and 5 M HF at a volume ratio of 1:1 for 30–60 s. In the next step, the c-Si substrates covered with Ag nanoparticles were immersed in a solution containing 5 M HF and 20% H₂O₂ at a volume ratio of 10:1 for 0.5–50 min. The immersion duration determined the thickness of the SiNW layer (see table 1). Later, the samples were rinsed several times in de-ionized water and dried at room temperature. Then, the SiNW arrays were rinsed in concentrated (65%) HNO₃ for 15 min to remove the residual Ag nanoparticles from the SiNWs. The structural properties of the SiNWs were studied using a Carl Zeiss Supra 40 scanning electron microscope (SEM).

The Raman scattering experiments were carried out using a Fourier-transform spectrometer (Bruker IFS 66v/S) equipped with a Raman scattering unit (FRA 106/S; excitation at 1064 nm). The maximum power of the laser radiation did not exceed 100 mW. Under the above-mentioned value, no significant heating of the samples took place. This was controlled by the ratio of the Stokes/anti-Stokes signals and the linear dependence of the Raman signal on excitation power.

Table 1. Thickness of SiNW layers formed for different etching times.

Etching time (min)	SiNW layer thickness (μm)
0.5	0.20
1.5	0.43
2.0	0.5
5	2.0
10	3.5
20	4.5
50	16



Figure 1. SEM image of a SiNW array recorded at a 70° tilt. The average nanowire height is 0.5 μm.

The TH generation was pumped by a quasi-cw Cr:forsterite laser (Avesta Project Ltd, 1250 nm, 80 fs, 150 mW, 80 MHz). The laser radiation was focused on the sample at an angle of incidence of 45° by a short-focus lens (FL = 14 mm), while the TH signal was collected by a lens with FL = 15 mm and NA = 0.6. KG3, and SS-15 filters were employed to select the TH signal (417 nm). A photon-counting tube (H7421, Hamamatsu) was used for the TH detection.

To estimate the photon lifetime, the above-mentioned Cr:forsterite laser and a Michelson interferometer with an oscillating mirror (oscillation frequency 0.1 Hz) were employed [26, 27]. A short-focus lens was set in the object shoulder of the interferometer to collect the light scattered by the sample. Analysis of the obtained cross-correlation functions was carried out accordingly [26–28].

3. Results and discussion

A typical SEM image for the formed SiNW array is shown in figure 1. The SiNWs are oriented perpendicular to the surface along the [100] crystallography direction (see the explanation in [11]). The diameter of the SiNWs ranges from 50 to 100 nm. The SiNW layer thickness increases monotonically with increased etching time (see table 1).

Figure 2(a) presents typical PL and Raman scattering spectra for the SiNWs. One can see a broad PL band that is typical of the interband transitions in c-Si [14, 16], and a sharp Stokes line at 520.5 cm⁻¹, corresponding to the phonon frequency in c-Si. The intensity of this Raman line was analyzed by subtracting the PL signal using OriginPro software. The pure Raman intensity for the samples with different thicknesses is shown in figure 2(b). The Raman signal values for all the

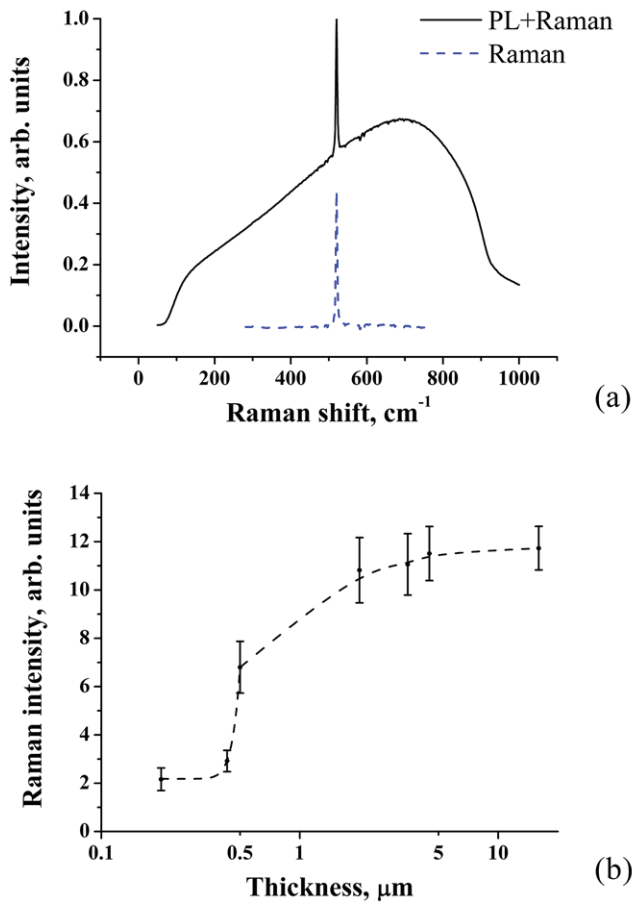


Figure 2. (a) Typical PL and Raman spectra for a SiNW array (thickness is $16 \mu\text{m}$). The Raman spectrum after the subtraction of the PL signal is shown separately (dashed line). The excitation wavelength is 1064 nm . (b) Raman intensity for line 520.5 cm^{-1} at different SiNW layer thicknesses. The intensity values are normalized to the Raman signal from c-Si. The dashed line is a guide to the eye.

samples were normalized to the Stokes component intensity for c-Si. For all the SiNW samples, the obtained Raman signals exceeded those from c-Si substrates. The increase of this dependence by up to $12 \times$ was observed. This dependence demonstrates the tendency to saturation at a thickness of more than $2 \mu\text{m}$.

A similar signal increase was obtained in previous works and is explained by the enlargement of the photon path in SiNW arrays caused by multiple scattering [14, 16, 17]. However, to the present day, an approximately fivefold increase of the Raman signal in comparison to that of the initial c-Si substrate is the largest that has been observed [17]. Here it is necessary to emphasize that we employ 20% hydrogen peroxide for the SiNW formation instead of the 30% used in the above-mentioned works. A smaller concentration of H_2O_2 most likely decreases the SiNW etching rate. This etching rate reduction may increase the surface area of the SiNWs and, as a result, the scattering cross-section will be greater. Hence the photon lifetime and the efficiency of the processes concerned with light scattering (for example, Raman scattering) increase.

The TH intensity dependence on SiNW layer thickness is shown in figure 3. Each TH signal from the SiNWs was

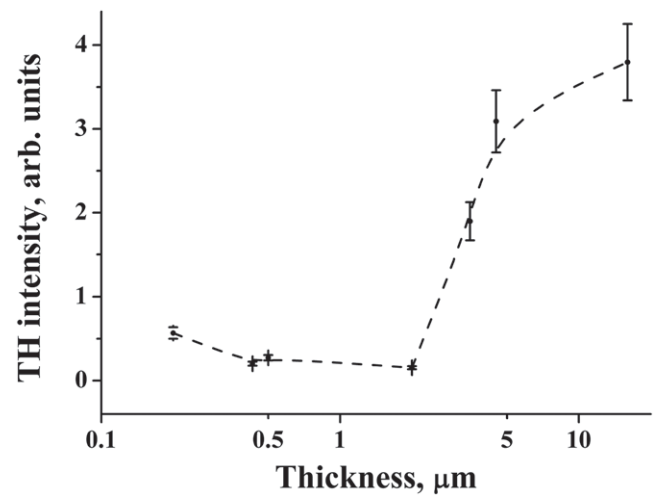


Figure 3. TH intensity at different SiNW layer thicknesses. The pump wavelength is 1250 nm . The intensity values are normalized to the TH signal for monocrystalline silicon. The dashed line is a guide to the eye.

normalized to one from c-Si. An important difference between the two types of signal is the presence of a diffuse scattered component in the former, while the latter only contains specular reflected TH. To avoid misunderstandings, in both cases the signals were collected by a short-focus lens with a high numerical aperture (see section 2). Thus the integral TH signals in the solid angle were registered in our experiments and included both specular and diffuse TH components.

The signal from the samples with a thickness of less than $2 \mu\text{m}$ was several times smaller than that for c-Si (figure 3). However, signal increases of up to $4 \times$ were registered for the larger thicknesses of the SiNW arrays.

The increase of both the Raman and the TH signals for rather thick SiNW layers can be explained by the increase of the photon lifetime in SiNW arrays. To verify this idea we measured the cross-correlation function of the laser pulse and the pulse scattered by the SiNW array. The variation of the measured cross-correlation functions with sample thickness is shown in figure 4.

The cross-correlation functions for the SiNW layers not exceeding $2 \mu\text{m}$ in thickness are almost identical to those obtained when a mirror is used instead of a SiNW sample, i.e. the autocorrelation function for the laser pulse (top graph in figure 4). This function is symmetrical along the timescale. The cross-correlation functions for samples with larger thicknesses possess asymmetry and demonstrate a longer duration in the positive timescale. The photon lifetime increases with increasing duration up to 0.9 ps . In our opinion, this effect is caused by multiple light scattering inside the mesoscopic structure [29].

In our experiments, the dependences of the Raman and TH signals on the SiNW thickness are qualitatively similar and indicate two regimes: a moderate increase or even decrease at a low thickness, and a significant increase with a tendency to saturation for a higher thickness. It is worth noting that the dependence of total reflectance on thickness for scattering media demonstrates the same behavior [30]. The latter regime is close to the diffuse light propagation and is established at a

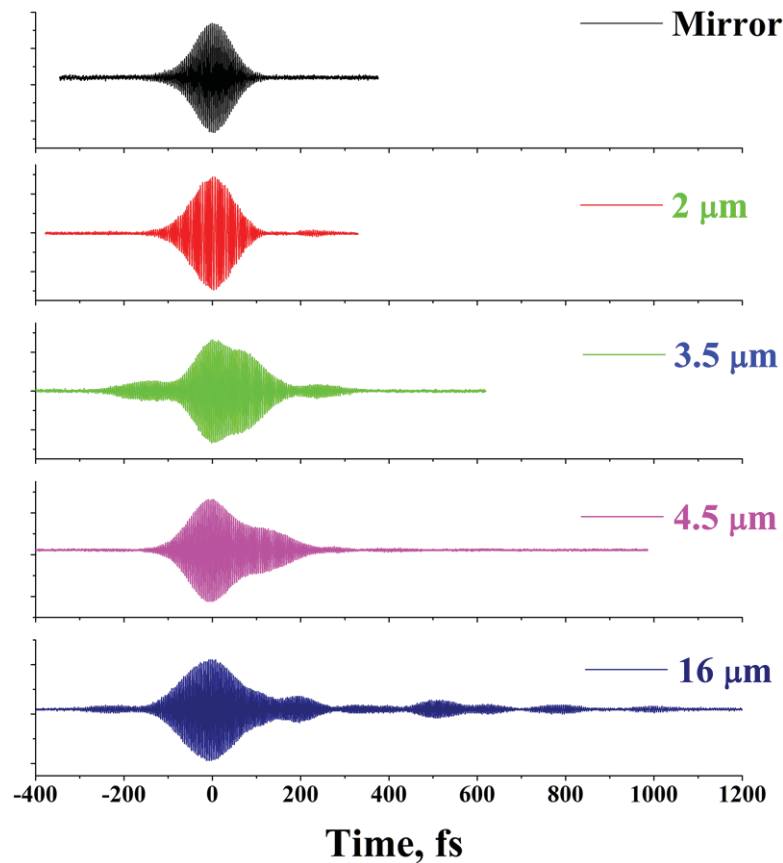


Figure 4. Cross-correlation functions for SiNW arrays of different thicknesses and an autocorrelation function (mirror instead of sample) for comparison. The pump wavelength is 1250 nm.

SiNW layer thickness above $2 \mu\text{m}$. Note that this layer thickness corresponds to the start of variations in cross-correlation functions. The increase of the SiNW layer thickness results in the increase of the photon lifetime inside the SiNW array, which brings about the increase of the Raman and TH signals due to the increase of the length of the light–matter interaction.

The greater enhancement of the Raman signal compared to the TH signal is caused by strong absorption of the latter. Indeed, at the TH wavelength (417 nm) c-Si possesses an absorption length of about $0.2 \mu\text{m}$ [31]. By contrast, for Raman scattering the Stokes component corresponds to 1126 nm, which is in the region of transparency. Taking into account the mesoscopic structure of the SiNW array, one can estimate that the TH photon transport length [29] hardly exceeds $1 \mu\text{m}$, limiting the length that the TH signal can be collected from. However, the diffuse light propagation is characterized by the rise of the total reflection with the sample increase, so the pump field intensity also increases, which in turn results in the enhancement of TH generation efficiency for the comparatively thick layers. It should be mentioned that a TH generation efficiency increase is observed in the SiNW arrays in comparison with bulk c-Si for the first time.

4. Conclusions

For the first time, the correlation between Raman and TH efficiency, cross-correlation function duration, and SiNW array

thickness is revealed. Direct measurements of the cross-correlation functions in the SiNW arrays show that the photon lifetime in such structures increases with increasing layer thickness because of multiple light scattering in the studied mesoscopic system.

Acknowledgments

The authors are grateful to A I Efimova for fruitful discussions. This work was carried out with financial support from the Russian Foundation for Basic Research (project 15-29-01185).

References

- [1] Lockwood D J and Pavesi L 2011 *Silicon Photonics II: Components and Integration* **119** 1–253
- [2] Yang P, Yan R and Fardy M 2010 *Nano Lett.* **10** 1529–36
- [3] Kelzenberg M D, Turner-Evans D B, Kayes B M, Filler M A, Putnam M C, Lewis N S and Atwater H A 2008 *Nano Lett.* **8** 710–4
- [4] Sivakov V, Andrä G, Gawlik A, Berger A, Plentz J, Falk F and Christiansen S H 2009 *Nano Lett.* **9** 1549–54
- [5] Lee H, Hong J, Lee S, Kim S-D, Kim Y-W and Lee T 2013 *Appl. Surf. Sci.* **274** 79–84
- [6] Huang Y, Duan X and Lieber C M 2005 *Small* **1** 142–7
- [7] Gan L, Sun L, He H and Ye Z 2014 *J. Mater. Chem. C* **2** 2668–73

- [8] Bronstrup G, Jahr N, Leiterer C, Csaki A, Fritzsche W and Christiansen S 2010 *ACS Nano* **4** 7113–22
- [9] Akihama Y and Hane K 2012 *Light: Sci. Appl.* **1** e16
- [10] Wagner R S and Ellis W C 1964 *Appl. Phys. Lett.* **4** 89–90
- [11] Sivakov V A, Bronstrup G, Pecz B, Berger A, Radnoczi G Z, Krause M and Christiansen S H 2010 *J. Phys. Chem. C* **114** 3798–803
- [12] Sivakov V A, Voigt F, Berger A, Bauer G and Christiansen S H 2010 *Phys. Rev. B* **82** 125446
- [13] Huang Z, Geyer N, Werner P, De Boor J and Gösele U 2011 *Adv. Mater.* **23** 285–308
- [14] Timoshenko V Yu, Gonchar K A, Golovan L A, Efimova A I, Sivakov V A, Dellith A and Christiansen S H 2011 *J. Nanoelectron. Optoelectron.* **6** 519–24
- [15] Gonchar K A, Osminkina L A, Galkin R A, Gongalsky M B, Marshov V S, Timoshenko V Yu, Kulmas M N, Solovyev V V, Kudryavtsev A A and Sivakov V A 2012 *J. Nanoelectron. Optoelectron.* **7** 602–6
- [16] Osminkina L A, Gonchar K A, Marshov V S, Bunkov K V, Petrov D V, Golovan L A, Talkenberg F, Sivakov V A and Timoshenko V Yu 2012 *Nanoscale Res. Lett.* **7** 524
- [17] Gonchar K A, Osminkina L A, Sivakov V, Lysenko V and Timoshenko V Yu 2014 *Semiconductors* **48** 1613–8
- [18] Kato S, Kurokawa Y, Watanabe Y, Yamada Y, Yamada A, Ohta Y, Niwa Y and Hirota M 2013 *Nanoscale Res. Lett.* **8** 216
- [19] Khorasaninejad M, Walia J and Saini S S 2012 *Nanotechnology* **23** 275706
- [20] Khorasaninejad M, Swillam M A, Pillai K and Saini S S 2012 *Opt. Lett.* **37** 4194–6
- [21] Wiecha P R, Arbouet A, Kallel H, Periwai P, Baron T and Paillard V 2015 *Phys. Rev. B* **91** 121416
- [22] Golovan L A, Gonchar K A, Timoshenko V Yu, Petrov G I and Yakovlev V V 2012 *Laser Phys. Lett.* **9** 145–50
- [23] Huang Z P, Wang R X, Jia D, Maoying L, Humphrey M G and Zhang C 2012 *ACS Appl. Mater. Interfaces* **4** 1553–9
- [24] Jung Y, Tong L, Tanaudommongkon A, Cheng J-X and Yang C 2009 *Nano Lett.* **9** 2440–4
- [25] Golovan L A, Kuznetsova L P, Fedotov A B, Konorov S O, Sidorov-Biryukov D A, Timoshenko V Yu, Zheltikov A M and Kashkarov P K 2003 *Appl. Phys. B* **76** 429–33
- [26] Golovan L A, Melnikov V A, Bestem'yanov K P, Zaboltnov S V, Gordienko V M, Timoshenko V Yu, Zheltikov A M and Kashkarov P K 2005 *Appl. Phys. B* **81** 353–6
- [27] Kashkarov P K et al 2005 *Phys. Solid State* **47** 159–65
- [28] Johnson P M, Imhof A, Bret B P J, Rivas J G and Lagendijk A 2003 *Phys. Rev. E* **68** 016604
- [29] Lagendijk A 1994 *Current Trends in Optics* ed J C Dainty (London: Academic) ch 4
- [30] Skipetrov S E and Chesnokov S S 1998 *Quantum Electron.* **28** 733–7
- [31] Jellison J E Jr and Modine F A 1982 *J. Appl. Phys.* **53** 3745–53